Delay- and topology-independent design for inducing amplitude death on networks with time-varying delay connections

Delay- and topology-independent design for inducing amplitude death on networks with time-varying delay connections

Yoshiki Sugitani,[1,2] Keiji Konishi,[1,*] and Naoyuki Hara[1]

[1]*Department of Electrical and Information Systems, Osaka Prefecture University, 1-1 Gakuen-cho, Naka-ku, Sakai, Osaka 599-8531, Japan*

[2]*Japan Society for the Promotion of Science, 5-3-1 Kojimachi, Chiyoda-ku, Tokyo 102-0083, Japan*

(Received 15 July 2015; published 30 October 2015)

We present a procedure to systematically design the connection parameters that will induce amplitude death in oscillator networks with time-varying delay connections. The parameters designed by the procedure are valid in oscillator networks with any network topology and with any connection delay. The validity of the design procedure is confirmed by numerical simulation. We also consider a partial time-varying delay connection, which has both time-invariant and time-varying delays. The effectiveness of the partial connection is shown theoretically and numerically.

DOI: 10.1103/PhysRevE.92.042928 PACS number(s): 05.45.Xt, 05.45.Gg, 02.30.Yy

I. INTRODUCTION

Collective behaviors in coupled oscillators have been of great interest in nonlinear sciences [1]. In one such behavior, namely amplitude death, a diffusive connection stabilizes an unstable steady state in a coupled oscillator [2,3]. Amplitude death has been observed in various systems, such as thermo-optical oscillators [4], the Belousov-Zhabotinsky reaction [5], electronic and biological oscillators [6], and the hair cells in the ear [7]. Although it has been well accepted that amplitude death cannot occur in *identical* oscillators with a diffusive connection [8,9], it has been shown that it can occur with a *delayed* diffusive connection [10,11]. Such death by delay has attracted much attention in nonlinear science, and it has been investigated both analytically and experimentally [12–26].

Employing amplitude death in engineering systems for the suppression of undesired oscillations has been reported for coupled laser systems [27], micropower grids [28], coupled permanent-magnet synchronous motors [29], and coupled thermoacoustic oscillators [30]. Hence, amplitude death is expected to have the potential to suppress undesired oscillations in various coupled systems. However, if the connection delay is much longer than the period of the undesired oscillation, then amplitude death cannot be induced [10]. This suggests that we are not able to use amplitude death in situations in which practical constraints require a long connection delay, such as when the undesired oscillations are far apart, or when the period of undesired oscillation is much shorter than the connection delay. To use amplitude death in such situations, a distributed-delay connection [31] and a multiple-delay connection [32] have been proposed. Unfortunately, it would be difficult to implement a distributed-delay connection in an engineering system, since the coupling signal needs to be integrated in real time, and a multiple-delay connection would increase the cost.

In a previous paper, we reported that a time-varying delay connection has the ability to cause amplitude death with a long connection delay [33]. Since this connection could be easily implemented and would not be expensive, it can be considered a strong candidate for use in engineering systems. This connection has been verified by experiments with electronic circuits [34]. Earlier studies [33,34] investigated only a pair of oscillators, but recently it was reported that a time-varying connection is also useful for oscillator networks [35,36].

From a practical point of view, we note that two problems remain for the time-varying delay connection. First, it is necessary to devise a systematic procedure for designing the connection parameters in order to avoid a burdensome trial-and-error process. In a previous study [33], we presented a delay-independent design procedure for the connection parameters for a pair of oscillators. However, to our knowledge, there is no such design procedure for oscillator networks [35,36]. Second, previous studies [35,36] assumed that it was necessary to vary all of the connection delays. This would be difficult and costly to implement for large-scale networks consisting of a huge number of oscillators.

The present paper tackles the above two problems. First, we show that a parametric approach in robust control theory provides a procedure to systematically design the connection parameters. The design procedure can be used for oscillator networks with any network topology and with any connection delay. As preparation for the design procedure, we analytically derive the stability regions for the various network topologies in the connection parameter space. Second, we propose a partial time-varying delay connection [37], which has both time-varying and time-invariant delays. Since our proposal requires that only some of the connection delays are varied, it would be easy and inexpensive to implement it for a large-scale network. The effectiveness of the partial time-varying delay connection is analytically and numerically confirmed. This paper is a substantially extended version of our conference papers [35,37].

The following notation is used throughout the present paper: $\arg[\mathsf{x}] \in [0,2\pi)$ denotes the principal argument of a complex number x.

II. COUPLED-OSCILLATOR NETWORK

Let us consider N Stuart-Landau oscillators (see Fig. 1),

$$\dot{Z}_j(t)=\{\mu+ia-|Z_j(t)|^2\}Z_j(t)+U_j(t) \quad (j=1,2,\ldots,N), \tag{1}$$

[*] http://www.eis.osakafu-u.ac.jp/~ecs

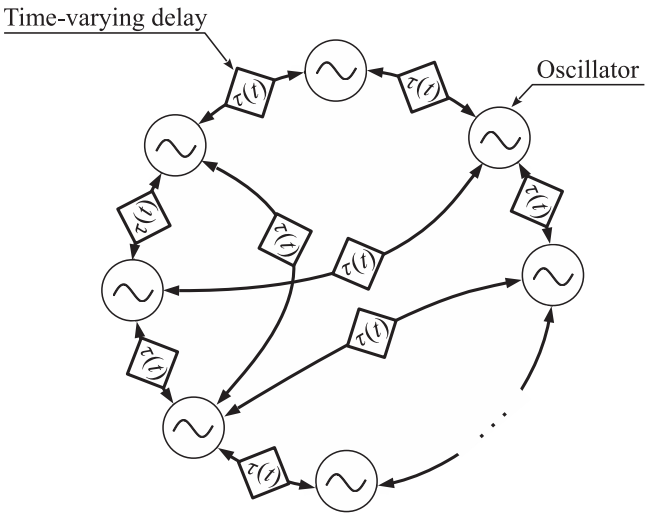

FIG. 1. Sketch of an oscillator network coupled by time-varying delay connections.

where $Z_j \in \mathbb{C}$ represents the state variable of oscillator j, and i is $\sqrt{-1}$. Each oscillator without a connection [i.e., $U_j(t) = 0$] has a fixed point $Z_j^* = 0$. The parameters $\mu > 0$ and $a > 0$, respectively, denote the instability of Z_j^* and the natural frequency of the oscillator. The coupling signal $U_j(t) \in \mathbb{C}$ can be written as

$$U_j(t) = k\left\{\frac{1}{d_j}\left(\sum_{l=1}^{N}\varepsilon_{jl}Z_{l,\tau}\right) - Z_j(t)\right\}, \tag{2}$$

where k is the coupling strength, $Z_{l,\tau} := Z_l[t-\tau(t)]$ is the delayed state variable, and ε_{jl} governs the network topology, as follows: $\varepsilon_{jl} = \varepsilon_{lj} = 1$ when oscillators j and l are connected, and 0 otherwise. Here, self-delayed feedback is not used, i.e., $\varepsilon_{jj} = 0$. The degree of oscillator j is given by $d_j := \sum_{l=1}^{N}\varepsilon_{jl}$. It should be noted that the present paper deals with oscillators of arbitrary degree $d_j > 0$, whereas a previous study [36] dealt only with oscillators of identical degree, $d_1 = d_2 = \cdots = d_N > 0$ (i.e., a regular network).

The connection delay $\tau(t) > 0$, as illustrated in Fig. 2, varies periodically around a nominal delay $\tau_0 > 0$:

$$\tau(t) := \tau_0 + \delta f(\Omega t), \tag{3}$$

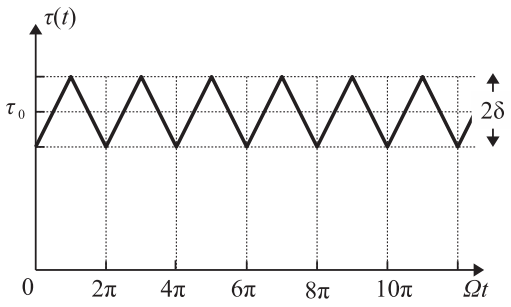

FIG. 2. Illustration of the time-varying delay function $\tau(t)$.

with amplitude[1] $\delta \in [0, \tau_0)$, frequency $\Omega > 0$, and a periodic sawtooth function [33,38,39]:

$$f(x) := \begin{cases} +\frac{2}{\pi}\left(x - \frac{\pi}{2} - 2n\pi\right) & \text{if } x \in [2n\pi,(2n+1)\pi), \\ -\frac{2}{\pi}\left(x - \frac{3\pi}{2} - 2n\pi\right) & \text{if } x \in [(2n+1)\pi,2(n+1)\pi) \end{cases}$$
$$(n = 0,1,2,\ldots).$$

The oscillators (1) coupled by Eq. (2) have a homogeneous steady state:

$$[Z_1^*, Z_2^*, \ldots, Z_N^*]^{\mathrm{T}} = [0,0,\ldots,0]^{\mathrm{T}}. \tag{4}$$

Let $z_j(t) := Z_j(t) - Z_j^*$ be a perturbation from the steady state (4). Then, the dynamics of the perturbation around this steady state can be described by

$$\dot{z}_j(t) = (\mu + ia)\, z_j(t) + k\left\{\frac{1}{d_j}\left(\sum_{l=1}^{N}\varepsilon_{jl}z_{l,\tau}\right) - z_j(t)\right\}$$
$$(j = 1,2,\ldots,N). \tag{5}$$

This linearized system (5) can be written as

$$\dot{\boldsymbol{X}}(t) = (\boldsymbol{I}_N \otimes \boldsymbol{A}_s)\boldsymbol{X}(t) + k(\boldsymbol{E} \otimes \boldsymbol{I}_2)\boldsymbol{X}[t-\tau(t)], \tag{6}$$

where

$$\boldsymbol{X}(t) := [\mathrm{Re}[z_1(t)],\mathrm{Im}[z_1(t)],\ldots,\mathrm{Re}[z_N(t)],\mathrm{Im}[z_N(t)]]^{\mathrm{T}},$$
$$\boldsymbol{A}_s := \boldsymbol{A} - k\boldsymbol{I}_2, \quad \boldsymbol{A} := \begin{bmatrix} \mu & -a \\ a & \mu \end{bmatrix}.$$

$\boldsymbol{I}_N$ is the N-dimensional unit matrix, and the matrix $\boldsymbol{E}$ governs the network topology; that is, its elements are given by $\{\boldsymbol{E}\}_{jl} = \varepsilon_{jl}/d_j$ $(l \neq j)$ and $\{\boldsymbol{E}\}_{jj} = 0$.

III. STABILITY ANALYSIS

We will show that the stability of the linear system (6) can be expressed as a simple characteristic equation. Furthermore, we will briefly illustrate how to draw the marginal stability curves, which will allow us to obtain amplitude death regions in the connection parameter space. Amplitude death regions will be drawn for various network topologies.

A. Linear stability analysis

The stability of this state (4) is difficult to analyze, since the linear system (6) has a time-varying delay. However, it has been reported [40] that the stability of the linear time-invariant system

$$\dot{\boldsymbol{X}}(t) = (\boldsymbol{I}_N \otimes \boldsymbol{A}_s)\boldsymbol{X}(t) + \frac{1}{2\delta}k(\boldsymbol{E} \otimes \boldsymbol{I}_2)\int_{t-\tau_0-\delta}^{t-\tau_0+\delta}\boldsymbol{X}(\theta)d\theta \tag{7}$$

is the same as that of the linear system (6) if Ω is sufficiently large compared to the oscillator frequency a. Thus, we can easily analyze the stability under the assumption $\Omega \gg a$. The characteristic function

$$G(s) = \det[s\boldsymbol{I}_{2N} - (\boldsymbol{I}_N \otimes \boldsymbol{A}_s) - k(\boldsymbol{E} \otimes \boldsymbol{I}_2)e^{-s\tau_0}H(s\delta)] \tag{8}$$

[1]Obviously, the delay amplitude δ must be less than the nominal delay τ_0.

determines the stability of this system (7), where

$$H(x) := \begin{cases} \dfrac{\sinh x}{x} & \text{if } x \neq 0, \\ 1 & \text{if } x = 0. \end{cases} \tag{9}$$

$\boldsymbol{I}_N - \boldsymbol{E}$ can be diagonalized as $\boldsymbol{T}^{-1}(\boldsymbol{I}_N - \boldsymbol{E})\boldsymbol{T} = \mathrm{diag}(\rho_1, \ldots, \rho_N)$ by using a transformation matrix[2] $\boldsymbol{T}$, where $\rho_p\,(p = 1, \ldots, N)$ are the eigenvalues of $\boldsymbol{I}_N - \boldsymbol{E}$. Hence, the characteristic function (8) can be written as

$$G(s) = \prod_{p=1}^{N} g(s, \rho_p), \tag{10}$$

where

$$\begin{aligned} g(s,\rho) :&= \det[s\boldsymbol{I}_2 - \boldsymbol{A}_s - k(1-\rho)\boldsymbol{I}_2 e^{-s\tau_0} H(s\delta)] \\ &= \{s - \mu + k - k(1-\rho)e^{-s\tau_0} H(s\delta)\}^2 + a^2. \end{aligned} \tag{11}$$

The form of this function (10) suggests that the stability of this state (4) is equal to that of the characteristic function (11) for $p = 1, 2, \ldots, N$. Note that the eigenvalues of $\boldsymbol{I}_N - \boldsymbol{E}$ always satisfy

$$0 = \rho_1 \leqslant \rho_2 \leqslant \cdots \leqslant \rho_N \leqslant 2 \tag{12}$$

for any network topology [41]. We obtain the stability region on the connection parameter space (k versus τ_0) by drawing the marginal stability curves in accordance with the procedure described in Appendix A.

B. Numerical examples

We will now draw the marginal stability curves in (k, τ_0) space for several networks. Throughout this paper, we will fix the parameters of the oscillators (1) and the frequency of Eq. (3) as

$$\mu = 0.5,\ a = \pi,\ \Omega = 10\pi. \tag{13}$$

Figure 3 shows the curves for four networks with different topologies ($N = 50$): ring topology ($\rho_1 = 0, \ldots, \rho_{50} = 2$), all-to-all topology ($\rho_1 = 0,\ \rho_2 = \rho_3 = \cdots = \rho_{50} = 50/49$), small-world topology with $N_c = 10$ short cuts ($\rho_1 = 0, \ldots, \rho_{50} = 1.988$), and scale-free topology ($\rho_1 = 0, \ldots, \rho_{50} = 1.7312$). Note that in networks with small-world and scale-free topologies, the oscillators are not of identical degree; thus, such situations were not considered in the previous study [36]. For each network, each of the four delay amplitudes $\delta = 0.15,\ 0.35,\ 0.50$, and 1.00 was employed. When a connection parameter set (k, τ_0) crosses the thin (bold) line with increasing k, a root s of $g(s,\rho) = 0$ cuts through the imaginary axis from left to right (right to left). Here, the shaded areas represent the stability regions where Eq. (10) has no roots in the right half of the complex plane.

For $\delta = 0.15$, as shown in Figs. 3(a), 3(e), 3(i), and 3(m), we see that the networks have small stability regions and that τ_0 is bounded above. An increase in δ is seen to enlarge the stability regions. In these regions, there is no upper bound on τ_0. For instance, in Fig. 3(p), the stability region has no upper bound on τ_0 in the range $k \in (0.500, 9.822)$. In other words, we can induce amplitude death for any connection delay τ_0 within this range of k. These results indicate that the time-varying delay connection is useful for inducing amplitude death not only in a pair of oscillators [33] but also in a larger network of oscillators.

[2]This is because $\boldsymbol{I}_N - \boldsymbol{E}$ and the real symmetric matrix $\boldsymbol{I}_N - \boldsymbol{D}^{-1/2}\boldsymbol{C}\boldsymbol{D}^{-1/2}$ are similar, where $\boldsymbol{D} := \mathrm{diag}(d_1, d_2, \ldots, d_N)$ and $\{\boldsymbol{C}\}_{jl} := \varepsilon_{jl}$ [41,42].

IV. DESIGN OF CONNECTION PARAMETERS

The stability region depends on the network topology, as illustrated in Fig. 3; thus, we notice that detailed information on network topology is inevitably required in order to design the connection parameters that will induce amplitude death. However, it would be difficult to obtain detailed information on the network topology in a real-world situation. Moreover, it would be difficult to estimate the connection delay, which might be very long due to practical constraints. Hence, in this section, we will provide a design procedure for the connection parameters so that the induction of amplitude death is independent of both the network topology and the connection delay.

From Eqs. (11) and (12), the topology-independent stability of the steady state (4) is equivalent to the stability of the family

$$\Sigma := \{g(s,\rho) \mid \rho \in [0,2]\}. \tag{14}$$

Here, $g(s,\rho)$ can be described by $g(s,\rho) = g^{(+)}(s,\rho)g^{(-)}(s,\rho)$, where

$$g^{(\pm)}(s,\rho) := s - \mu + k - k(1-\rho)e^{-s\tau_0} H(s\delta) \pm ia.$$

It can be easily confirmed that $g^{(-)}(s,\rho) = 0$ and $g^{(+)}(s,\rho) = 0$ only have roots with the same real parts. Hence, instead of $g(s,\rho)$, it is enough to analyze the stability of $g^{(-)}(s,\rho)$: the stability of Σ can be reduced to that of

$$\Sigma_{(-)} := \{g^{(-)}(s,\rho) \mid \rho \in [0,2]\}. \tag{15}$$

Moreover, $\Sigma_{(-)}$ can be described by the segment

$$\Sigma_{(-)} = \{\hat{g}(s,\eta) := (1-\eta)g^{(-)}(s,0) + \eta g^{(-)}(s,2) | \eta \in [0,1]\}, \tag{16}$$

which has end points at $g^{(-)}(s,0)$ and $g^{(-)}(s,2)$. As a consequence, the stability of the steady state (4) is guaranteed independently of the network topology if $\Sigma_{(-)}$ is stable; however, in general, it is difficult to guarantee the stability of $\hat{g}(s,\eta)$ for all $\eta \in [0,1]$.

A parametric approach in robust control theory provides an easy way to guarantee the stability of $\Sigma_{(-)}$.

Theorem 1. Assume that $\mu - k < 0$ holds. The segment $\Sigma_{(-)}$, $\hat{g}(s,\eta)$ for all $\eta \in [0,1]$, is stable if the following two conditions hold:

(a) $\hat{g}(s,\eta)$ is stable for both $\eta = 0$ and 1.

(b) $\psi(\omega) := \arg[\hat{g}(i\omega,0)] - \arg[\hat{g}(i\omega,1)] \neq \pm\pi,\ \forall\omega \in \mathbb{R}$.

Proof. See Appendix B.

Condition (a) implies that for $\eta = 0$ and 1, $\hat{g}(s,\eta) = 0$ has only roots with negative real parts. Condition (b) implies that these roots stay in the open left half of the complex plane, despite the variation in η.

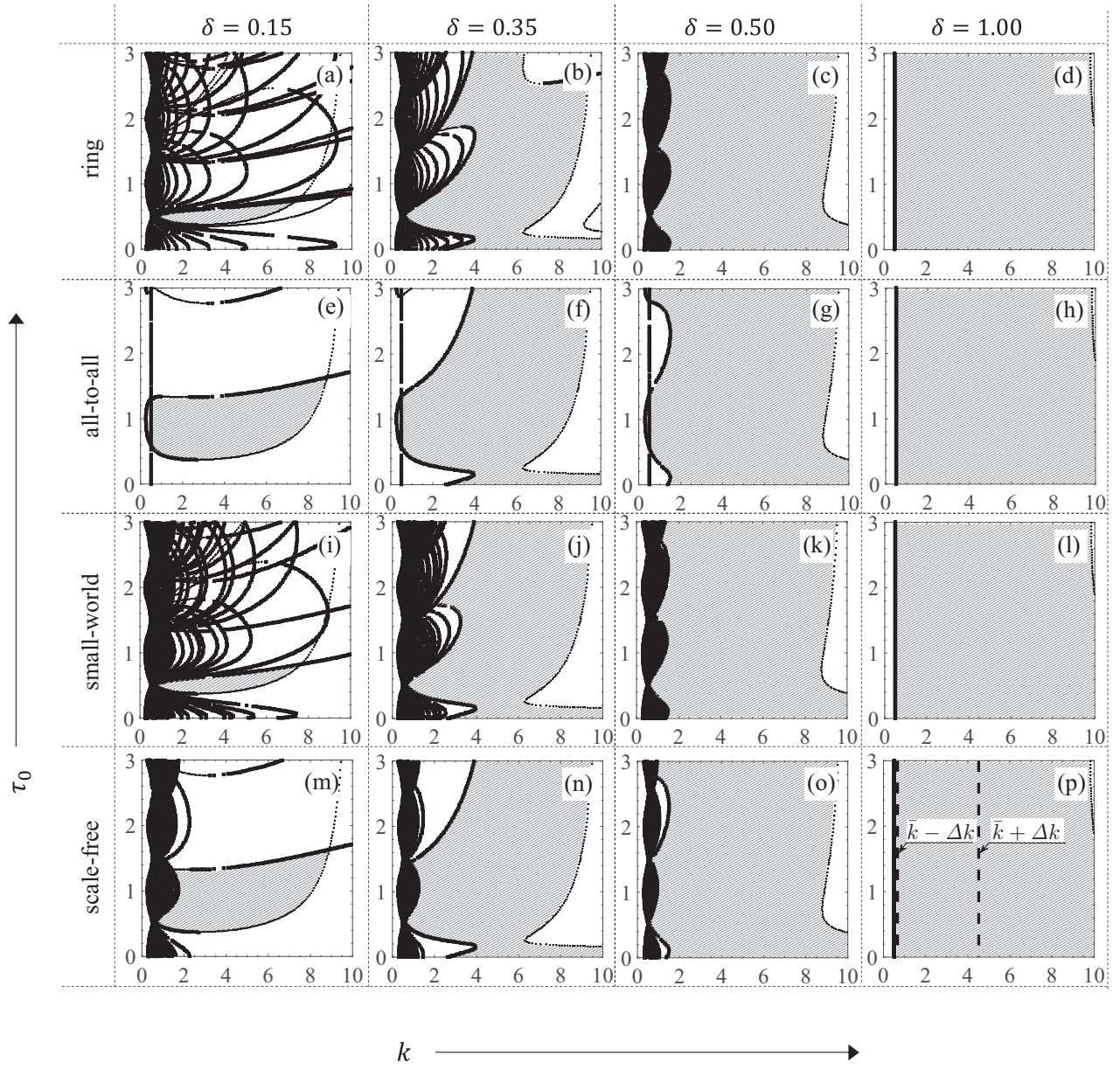

FIG. 3. Stability regions in (k,τ_0) space for four different network topologies ($N = 50$): (a)–(d) ring topology, (e)–(h) all-to-all topology, (i)–(l) small-world topology with $N_c = 10$ short cuts, and (m)–(p) scale-free network topology. Delay amplitudes are $\delta = 0.15$, 0.35, 0.50, and 1.00, as indicated for each column. The curves and shaded areas show the solutions of $g(i\lambda,\rho) = 0$ and the stability regions, respectively.

In preparation for designing connection parameters for oscillator networks (i.e., $N > 2$), we will review our results for the case of $N = 2$ [33]. Because the stability of the steady state (4) with $N = 2$ is governed by only $\hat{g}(s,0)$ and $\hat{g}(s,1)$, it is enough to consider condition (a), as follows.

Lemma 1 [33]. Assume that the oscillators (1) satisfy

$$\mu < \frac{a(2+\pi)}{4\pi}, \tag{17}$$

and the frequency variation Ω is sufficiently large (i.e., $\Omega \gg a$). The characteristic function $\hat{g}(s,\eta)$ is stable both for $\eta = 0$ and 1 for an arbitrarily long nominal delay τ_0, if the delay amplitude is set to

$$\delta = \pi/a, \tag{18}$$

and the coupling strength is set such that

$$k \in (\bar{k} - \Delta k, \bar{k} + \Delta k), \tag{19}$$

where

$$\bar{k} := \left(\frac{2+\pi}{2\pi}\right)a, \quad \Delta k := \frac{1}{2\pi}\sqrt{a(2+\pi)\{a(2+\pi) - 4\pi\mu\}}. \tag{20}$$

On the basis of our previous study, we will propose a procedure for designing oscillator networks (i.e., $N > 2$). It is obvious that our design must satisfy both conditions (a) and (b). We now show that the connection parameters designed according to Lemma 1 also satisfy condition (b).

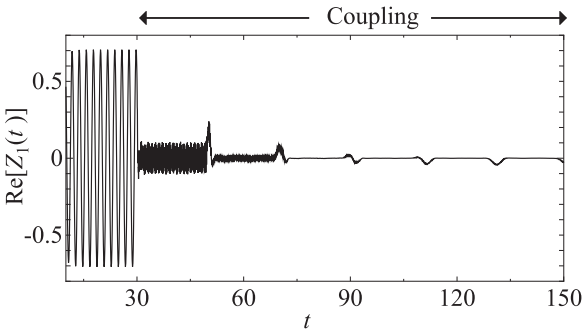

FIG. 4. Time-series data of Re$[Z_1(t)]$ ($k = 2.5, \delta = 1.00, \tau_0 = 20$).

Lemma 2. Assume that the oscillators (1) satisfy the inequality (17) of Lemma 1. The condition $\psi(\omega) \neq \pm\pi, \forall\omega \in \mathbb{R}$ [i.e., condition (b) in Theorem 1] holds if the connection parameters δ and k are designed according to Lemma 1.

Proof. See Appendix C.

As a result, both conditions (a) and (b) are satisfied if the connection parameters are designed according to Lemma 1. Moreover, we see that under assumption (17), the coupling strength k designed according to Lemma 1 satisfies the assumption of Theorem 1 (i.e., $\mu - k < 0$; see Appendix D). From these facts, we can now provide a systematic procedure for designing oscillator networks.

Theorem 2. Assume that the inequality (17) holds for the oscillators (1), and assume that the frequency variation Ω in the connection (2) is sufficiently large (i.e., $\Omega \gg a$). The steady state (4) is stable for the arbitrary nominal delay τ_0, for any number of oscillators N, and for any network topology $\boldsymbol{E}$, if the delay amplitude δ and the coupling strength k are set in accordance with Eq. (18) and the range of Eq. (19), respectively.

Proof. We omit the proof, as it is obvious from Theorem 1 and Lemmas 1 and 2.

We will now design the connection parameters in accordance with Theorem 2 for the parameter values given in Eq. (13). In this case, Ω is sufficiently large, and the assumption (17) given in Lemma 1 holds; then, $\delta = 1.00$ and $k \in (0.561, 4.580)$ are designed by Eqs. (18) and (19), respectively. The stability region of the scale-free network ($N = 50$) with the parameters designed by this procedure is shown in Fig. 3(p). The area between the dotted lines represents the designed range (19). As can be seen, this range (19) lies in the stability region. The time series for oscillator 1 in the scale-free network is shown in Fig. 4. At $t = 30$, all the oscillators are coupled with the designed connection parameters $\delta = 1.00$ and $k = 2.5$. This result indicates that the designed connection induces amplitude death after coupling, even for a long connection delay of $\tau_0 = 20$.

From an engineering point of view, the robustness of our procedure against parameter errors and noise should be considered. In real systems, it is difficult to set δ to be exactly according to Eq. (18); δ inevitably has small errors away from Eq. (18). We have numerically confirmed at parameters (13) that, even if δ has errors within $\pm 5\%$ away from Eq. (18), the stability of the steady state remains when condition (19) holds. Thus, we may say that our procedure would be robust against small errors away from Eq. (18). Furthermore, noise is inevitably present in the real world. We have numerically confirmed that designed parameters can induce amplitude death even in the situation in which a small random signal within $[-3 \times 10^{-3}, 3 \times 10^{-3}]$ is added to all the oscillators. Therefore, we may also say that our procedure would be robust against small noise.

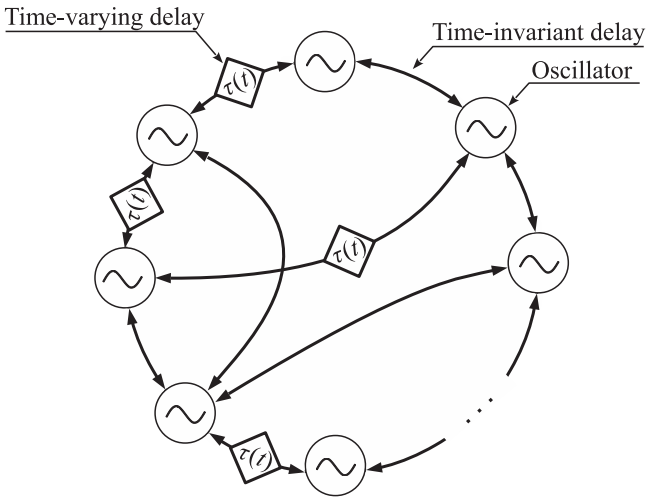

FIG. 5. Sketch of an oscillator network coupled by a partial time-varying delay connection.

V. PARTIAL TIME-VARYING DELAY CONNECTION

In the previous sections, we analytically and numerically showed that a time-varying delay connection is useful for inducing amplitude death in various network topologies. However, for large-scale networks with a huge number of oscillators, it would be difficult to apply a high-frequency variance to all of the connection delays. Therefore, in this section, we propose a partial time-varying delay connection (see Fig. 5), in which some connection delays are varied and the others are held constant. This is done because a partial time-varying delay connection is obviously easier to implement than a conventional time-varying delay connection. From an engineering viewpoint, it is necessary to know how many and which delays should be varied for inducing amplitude death. In this section, we will investigate how the number of time-varying delays and their configuration influence amplitude death.

We consider an oscillator network with a partial time-varying delay connection. Instead of Eq. (2), we will use the coupling signal $U_j(t)$ of the oscillators (1):

$$U_j(t) = k\left[\frac{1}{\tilde{d}_j}\left\{\sum_{l=1}^{N}\left(v_{jl}Z_{l,\tau} + w_{jl}Z_{l,\tau_0}\right)\right\} - Z_j(t)\right], \quad (21)$$

where $Z_{l,\tau} := Z_l[t - \tau(t)]$ and $Z_{l,\tau_0} := Z_l(t - \tau_0)$ denote the time-varying and time-invariant delayed signals, respectively, and v_{jl} and w_{jl} govern the network topology, as follows: $v_{jl} = v_{lj} = 1$ ($w_{jl} = w_{lj} = 1$) denotes that oscillators j and l are connected by a time-varying (time-invariant) delay connection; otherwise $v_{jl} = v_{lj} = 0$ ($w_{jl} = w_{lj} = 0$). Time-varying and time-invariant connections (i.e., $v_{jl} = w_{jl} = 1$)

are not employed in parallel (i.e., $v_{jl}w_{jl} = 0, \forall j,l$). The degree of oscillator j is defined by $\tilde{d}_j := \sum_{l=1}^{N}(v_{jl} + w_{jl})$.

A. Linear stability analysis

The oscillators (1) coupled by this connection (21) have a steady state (4). Linearizing Eq. (1) with Eq. (21) around this steady state (4), we obtain the linear system

$$\dot{\boldsymbol{X}}(t) = (\boldsymbol{I}_N \otimes \boldsymbol{A}_s)\boldsymbol{X}(t) + k\{(\boldsymbol{V} \otimes \boldsymbol{I}_2)\boldsymbol{X}_{\tau(t)} + (\boldsymbol{W} \otimes \boldsymbol{I}_2)\boldsymbol{X}_{\tau_0}\}. \tag{22}$$

The elements of $\boldsymbol{V}$ and $\boldsymbol{W}$ are given by $\{\boldsymbol{V}\}_{jl} = v_{jl}/\tilde{d}_j$ and $\{\boldsymbol{W}\}_{jl} = w_{jl}/\tilde{d}_j$, respectively. Assume that Ω is sufficiently large compared with the oscillator frequency a; then the stability of the time-varying system (22) is equivalent to that of the following time-invariant system [40]:

$$\dot{\boldsymbol{X}}(t) = (\boldsymbol{I}_N \otimes \boldsymbol{A}_s)\boldsymbol{X}(t) + k\left\{\frac{(\boldsymbol{V} \otimes \boldsymbol{I}_2)}{2\delta}\int_{t-\tau_0-\delta}^{t-\tau_0+\delta}\boldsymbol{X}(\theta)d\theta + (\boldsymbol{W} \otimes \boldsymbol{I}_2)\boldsymbol{X}_{\tau_0}\right\}. \tag{23}$$

The characteristic function of this time-invariant system (23) is given by

$$\tilde{G}(s) = \det[s\boldsymbol{I}_{2N} - (\boldsymbol{I}_N \otimes \boldsymbol{A}_s) - k\{\boldsymbol{M}(s) \otimes \boldsymbol{I}_2\}e^{-s\tau_0}], \tag{24}$$

where $\boldsymbol{M}(s) := \boldsymbol{V}H(s\delta) + \boldsymbol{W}$. The stability of the steady state (4) is equal to that of Eq. (24). We shall give the procedure for deriving the marginal stability curve. Substituting $s = i\lambda$ ($\lambda \in \mathbb{R}$) into Eq. (24), we obtain

$$\tilde{G}(i\lambda) = \det[i\lambda\boldsymbol{I}_{2N} - (\boldsymbol{I}_N \otimes \boldsymbol{A}_s) - k\{\tilde{\boldsymbol{M}}(\lambda) \otimes \boldsymbol{I}_2\}e^{-i\lambda\tau_0}], \tag{25}$$

where $\tilde{\boldsymbol{M}}(\lambda) := \boldsymbol{M}(i\lambda) = \boldsymbol{V}\Phi(\lambda\delta) + \boldsymbol{W}$. Here, $\Phi(x)$ is defined by Eq. (A2) in Appendix A. The connection matrix $\tilde{\boldsymbol{M}}(\lambda)$ can be diagonalized[3] as $\boldsymbol{T}^{-1}\tilde{\boldsymbol{M}}(\lambda)\boldsymbol{T} = \mathrm{diag}\{\tilde{\rho}_1(\lambda), \tilde{\rho}_2(\lambda), \ldots, \tilde{\rho}_N(\lambda)\}$ by a transformation matrix $\boldsymbol{T}$, where $\tilde{\rho}_p(\lambda)(p = 1, \ldots, N)$ are the eigenvalues of $\tilde{\boldsymbol{M}}(\lambda)$. We note that the eigenvalues $\tilde{\rho}(\lambda)$ are functions of λ, since $\tilde{\boldsymbol{M}}(\lambda)$ includes $\Phi(\lambda\delta)$. As a consequence, Eq. (25) can be written as follows:

$$\tilde{G}(i\lambda) = \prod_{p=1}^{N}\tilde{g}(i\lambda, \tilde{\rho}_p(\lambda)),$$

where

$$\tilde{g}(i\lambda, \tilde{\rho}(\lambda)) := [i\lambda - \mu + k\{1 - \tilde{\rho}(\lambda)e^{-i\lambda\tau_0}\}]^2 + a^2. \tag{26}$$

Separating Eq. (26) into real and imaginary parts, we can analytically derive the marginal stability curves by using the procedure described in Appendix A.

[3]This is obvious from the similarity of $\tilde{\boldsymbol{M}}(\lambda)$ and the real symmetric matrix $\tilde{\boldsymbol{D}}^{1/2}\tilde{\boldsymbol{M}}(\lambda)\tilde{\boldsymbol{D}}^{-1/2}$, with $\tilde{\boldsymbol{D}} := \mathrm{diag}(\tilde{d}_1, \tilde{d}_2, \ldots, \tilde{d}_N)$.

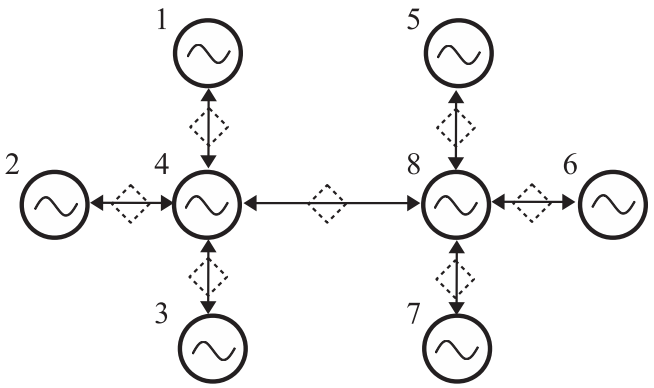

FIG. 6. Oscillator network ($N = 8$).

B. Numerical example

For a numerical example, we consider the network of $N = 8$ coupled oscillators shown in Fig. 6. In this network, two oscillators are of high degree (i.e., $\tilde{d}_4 = \tilde{d}_8 = 4$), and we will call them *hub oscillators*; six oscillators are of low degree (i.e., $\tilde{d}_1 = \tilde{d}_2 = \tilde{d}_3 = \tilde{d}_5 = \tilde{d}_6 = \tilde{d}_7 = 1$), and we will call them *nonhub oscillators*.

We will investigate how the number of time-varying delays and their configuration influence amplitude death. For this purpose, the following situations are considered: one (two) connection delay(s) is (are) varied, and the others are held constant. The parameters of the oscillators (1) are fixed as in Eq. (13), and the delay amplitude is set to $\delta = 1.00$. Note that, for these parameters, the conventional time-varying delay connection has large stability regions, and this is independent of the network topology, as can be seen in Figs. 3(d), 3(h), 3(l), and 3(p).

1. *One time-varying delay connection*

Here, we deal with the situation in which one connection delay is varied and the other six connection delays are held constant. We will use the notation $i \sim j$ to indicate that the connection delay between oscillators i and j is varied. The following two cases can be considered: (a) a nonhub $\sim$ hub connection, and (b) a hub $\sim$ hub connection (i.e., $4 \sim 8$). Now $2 \sim 4$, without loss of generality, is employed for case (a).

The stability region for case (a) is shown in Fig. 7(a), and that for case (b) is shown in Fig. 7(b). In Fig. 7(a), amplitude death is never induced, since the nominal delay τ_0 in Eq. (3) must be greater than the delay amplitude $\delta = 1.00$. In contrast, Fig. 7(b) has a large stability region. The above results imply that, for one time-varying delay connection, the connection delay between the two hub oscillators should be varied in order to enlarge a stability region.

2. *Two time-varying delay connections*

Here, we deal with a situation in which two connection delays are varied and the other five are held constant. The following three cases can be considered: (a) two nonhub $\sim$ hub connections on the left or right side, as shown in Fig. 8(a); (b) a nonhub $\sim$ hub connection and a hub $\sim$ hub connection, as shown in Fig. 8(b); and (c) nonhub $\sim$ hub connections on both sides, as shown in Fig. 8(c). We choose, without loss of

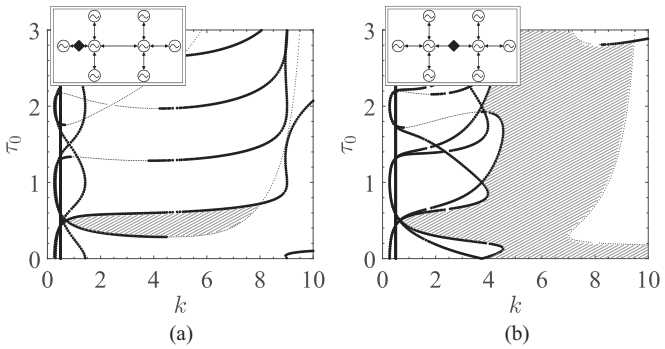

FIG. 7. Stability region for the network in Fig. 6 with one time-varying delay connection: (a) nonhub $\sim$ hub, (b) hub $\sim$ hub. The time-varying delay connection is denoted by a black diamond. The delay amplitude is $\delta = 1.00$.

generality, $1 \sim 4$ and $2 \sim 4$ for case (a), $2 \sim 4$ and $4 \sim 8$ for case (b), and $2 \sim 4$ and $6 \sim 8$ for case (c). The stability regions for cases (a), (b), and (c) are shown in Figs. 8(a), 8(b), and 8(c), respectively. For all the cases, we can induce amplitude death for a long connection delay τ_0. Furthermore, we can see that Fig. 8(a) has a smaller region than Fig. 8(b), which may lead us to think that the most important connection for expanding the region is the one between the two hub oscillators, as is the case in Fig. 7(b); however, this is not always true. The region in Fig. 8(c) is a little larger than that in Fig. 8(b), even though the connection delay between the two hub oscillators is not varied.

3. *Large network*

In the previous subsection, we showed that, for a large stability region, not only is the hub oscillator important, but so is the spatial distribution of the time-varying delays. Although we considered only a small network ($N = 8$), in this subsection we will further investigate how the spatial distribution of the time-varying delays influences the stability of large networks. For large N, it is difficult to analytically derive the stability region, since it is difficult to estimate the eigenvalue $\tilde{\rho}$ in Eq. (26); therefore, we will numerically estimate the stability region.

We will examine the influence of the spatial distribution of the time-varying delays. For this purpose, we will consider a ring network ($N = 20$) where each oscillator has the same degree (i.e., there is no hub oscillator). We focus on the situation in which 10 connection delays are varied, and the others are held constant. The following three distributions of time-varying delays are used, as shown in Fig. 9: (a) a random distribution, (b) a concentrated distribution, and (c) a uniform distribution.

Figures 10(a), 10(b), and 10(c), respectively, show the stability region of the networks in Figs. 9(a), 9(b), and 9(c) with $\delta = 1.00$ and the parameters stated in Eq. (13). The dots denote the stable parameter set[4] (k, τ_0). In spite of having the same numbers of time-varying delays, the stability regions

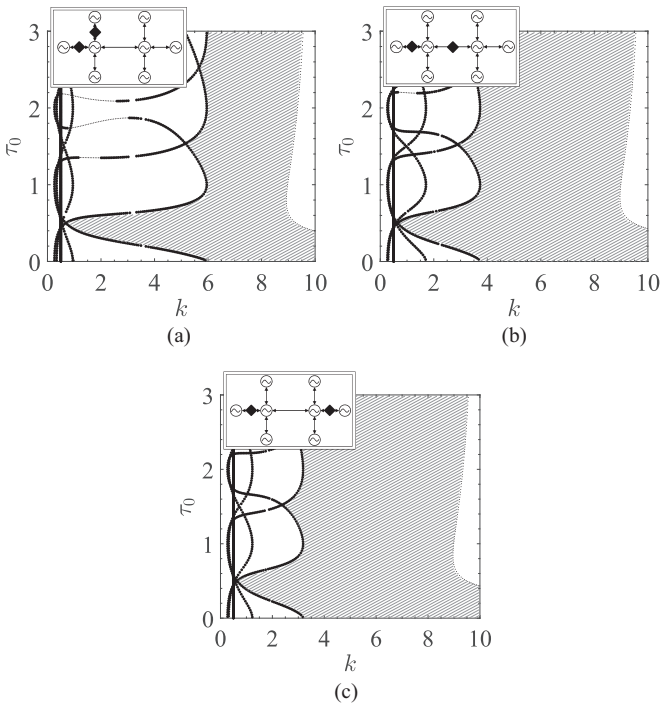

FIG. 8. Stability region for the network in Fig. 6 with two time-varying delay connections: (a) two nonhub $\sim$ hub on the left, (b) nonhub $\sim$ hub and hub $\sim$ hub, (c) nonhub $\sim$ hub on both sides. The time-varying delay connections are denoted by a black diamond. The delay amplitude is $\delta = 1.00$.

differ greatly. Figure 10(c) has the largest stability region, and Fig. 10(b) has no stability region. From these figures, it is conjectured that the network with uniformly distributed time-varying delays has a larger stability region than that with concentrated time-varying delays.[5] This conjecture does not contradict the results that we obtained for a small network ($N = 8$; see Fig. 8). We note that, for practical purposes, it is more useful to have a large stability region, and these results imply that, to achieve this, the time-varying delays should not be concentrated.

Note that we have confirmed that, for the uniform distribution, the stability region becomes small as the number of time-varying delay connections decreases, and the region vanishes at a critical number. From an engineering point of view, it is important to know this critical number in order to implement the partial time-varying delay connection inexpensively and easily. Estimation of the critical number is an open problem.

[4]The local stability is judged by the following procedure: the initial states of all the oscillators over the time interval $[-\tau_0 - \delta, 0]$ are uniformly and randomly chosen from the range $(-0.01, 0.01)$; all the oscillators run from the initial states; if all the oscillators satisfy $|Z_i(t) - Z_i^*| < 0.003, \forall t \in [1950, 2000]$ for $i = 1, 2, \ldots, N$, then the steady state is regarded as stable.

[5]We also have numerically investigated the uniform and concentrated distributions in the following three networks: $N = 30$ with 15 time-varying delay connections, $N = 40$ with 20, and $N = 50$ with 25. The same as shown in Fig. 10, large stability regions were obtained for the uniform distribution, and no stability region was obtained for the concentrated distribution.

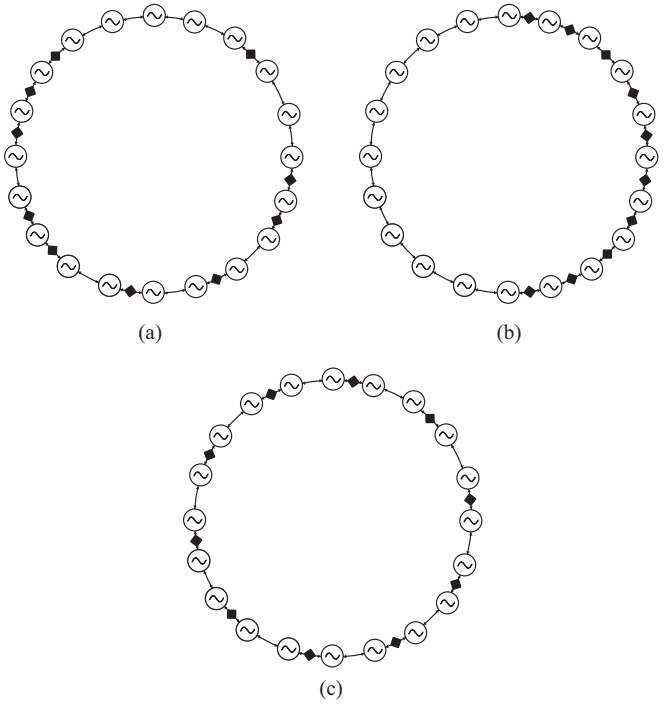

FIG. 9. Three types of configurations of time-varying delay connections ($N = 20$): (a) random distribution, (b) concentrated distribution, and (c) uniform distribution.

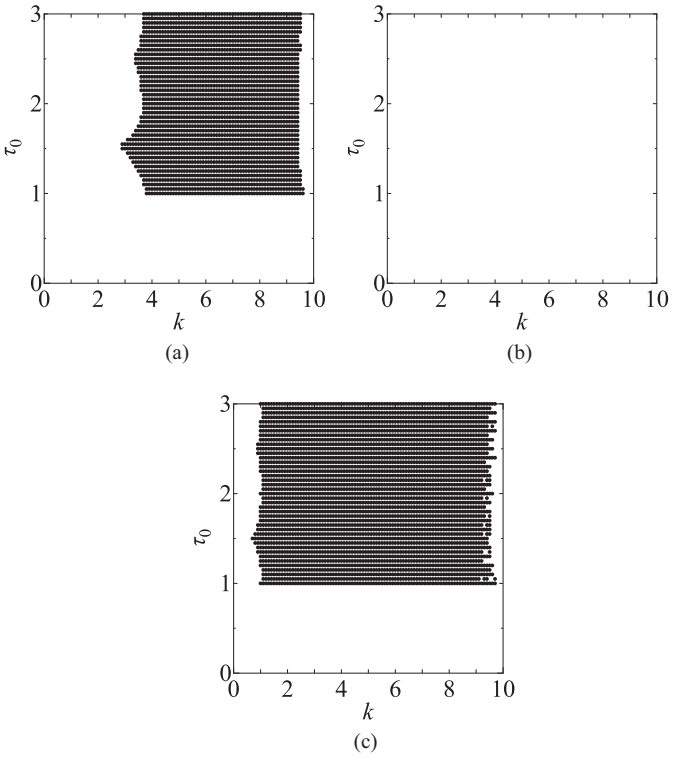

FIG. 10. Stability regions of the networks illustrated in Fig. 9: (a) random distribution, (b) concentrated distribution, and (c) uniform distribution.

VI. DISCUSSION

We will now review the details of the previous studies that dealt with using a time-varying delay to stabilize the steady states of oscillators and networks. In the earliest studies, a time-varying delay was used in the delayed feedback control of a single oscillator [38,39,44]; this allowed the stabilization of steady states with a longer feedback delay than could be stabilized by the original (i.e., time-invariant) delayed feedback control [45]. A feedback control system with time-varying delay was extended to two oscillators with a time-varying delay connection [33], and this connection with an arbitrarily long delay can cause amplitude death; this phenomenon was verified with experiments using electronic circuits [34]. These previous studies [33,34] investigated only a pair of oscillators. More recently, it was shown that the time-varying delay connection is also useful for oscillator networks [35,36]. In a previous study [35], we investigated the stability regions for various network topologies. Gjurchinovski *et al.* investigated the stability regions for different types of time-varying delay functions, including sawtooth, square, and sine functions [36], but they considered oscillators of the same degree. Furthermore, those studies [35,36] did not provide a design procedure of the connection parameters. In the present paper, we consider oscillators of differing degree, and we show a procedure to systematically design the connection parameters.

The parametric approach of robust control theory, which is used for deriving the design procedure (i.e., Theorem 2), is the key to the present paper. This approach has been used in our three papers [25,46,47]. Here, we will compare these papers with the present study. The first paper [46] provided a design of a high-dimensional oscillator network with a dynamic connection. As the dynamic connection does not contain a time delay, the characteristic equation is given by a polynomial. Thus, the design procedure was based on the Segment Lemma or Kharitonov's Theorem. The second paper [25] investigated a time-delayed oscillator network with a time-delayed connection: the oscillators and their connection contained time-invariant delays. The third paper [47] dealt with high-dimensional oscillators coupled by a time-invariant delay connection. In the second and third papers [25,47], the characteristic equation was given by a quasipolynomial due to the time delay, and design procedures based on a condition similar to condition (b) of Theorem 1 in the present study were provided. In the present study, we deal with two-dimensional oscillators coupled by a time-varying delay connection. The characteristic equation is more complex than that of previous studies [25,47], since the equation is given by a quasipolynomial with the nonlinear function (9). Our design procedure is provided on the basis of condition (b) of Theorem 1. As we showed above, the parametric approach can be used in various oscillator networks. It should be emphasized that there would still be great potential for the application of robust control theory, including the parametric approach, to network science.

VII. CONCLUSION

This paper investigated amplitude death in a coupled oscillator network with a time-varying delay connection. A parametric approach in robust control theory provided a

procedure for designing connection parameters that would induce amplitude death, independent of the connection delay and the network topology. We also proposed a partial time-varying delay connection, and the effectiveness of this connection was verified theoretically and numerically.

ACKNOWLEDGMENTS

The present research was partially supported by JSPS KAKENHI (26289131) and a Grant-in-Aid for JSPS Fellows (26·7041).

APPENDIX A: PROCEDURE FOR DERIVING THE MARGINAL STABILITY CURVES

Substituting $s = i\lambda$, where $\lambda \in \mathbb{R}$, into $g(s,\rho) = 0$, we can separate $g(s,\rho) = 0$ into its real and imaginary parts,

$$\begin{aligned} k - \mu - k(1-\rho)\Phi(\lambda\delta)\cos(\lambda\tau_0) &= 0, \\ \lambda - a + k(1-\rho)\Phi(\lambda\delta)\sin(\lambda\tau_0) &= 0, \end{aligned} \tag{A1}$$

where

$$\Phi(x) := \begin{cases} \frac{\sin x}{x} & \text{if } x \neq 0, \\ 1 & \text{if } x = 0. \end{cases} \tag{A2}$$

Eliminating τ_0 from Eq. (A1), we have

$$\{1-(1-\rho)^2\Phi^2(\lambda\delta)\}k^2 - 2\mu k + \mu^2 + (\lambda - a)^2 = 0. \tag{A3}$$

From Eq. (A3), the marginal stability curves of $g(s,\rho) = 0$ can be derived using the procedure proposed in our previous papers [33,35].

APPENDIX B: PROOF OF THEOREM 1

A previous study provided the stability condition, which was similar to Theorem 1, for the segment of polynomials and of quasipolynomials (see Lemmas 2.1 and 2.2 in [43]). In contrast, the segment $\Sigma_{(-)}$ belongs to neither the polynomials nor the quasipolynomials, since $\hat{g}(s,\eta)$ contains $H(x)$, as defined by Eq. (9). However, the boundary crossing theorem will help us to prove Theorem 1, as in the same previous study [43].

It is obvious that the stability of the segment $\Sigma_{(-)}$ is guaranteed if the following conditions hold: (i) both ends of the segment are stable; and (ii) the roots of $\hat{g}(s,\eta) = 0$ never move to the right half-plane for any $\eta \in [0,1]$. Although condition (i) is obviously the same as condition (a), it is not easy to see that condition (ii) is the same as condition (b). Therefore, we will focus on condition (ii).

We will consider the stability of $\hat{g}(s,\eta)$ separately for $\eta = 1/2$ and $\eta \in [0,1/2) \cup (1/2,1]$, since for $\eta = 1/2$, $\hat{g}(s,\eta)$ is a first-degree polynomial, but for $\eta \in [0,1/2) \cup (1/2,1]$, it is not a polynomial. For $\eta = 1/2$, we see that $\hat{g}(s,\eta) = 0$ has only one root, $s = \mu - k + ia$, and this root has negative real parts due to the assumption that $\mu - k < 0$. For $\eta \in [0,1/2) \cup (1/2,1]$, the roots of $\hat{g}(s,\eta) = 0$ never move to the right half-plane if no roots of $\hat{g}(s,\eta) = 0$ cross the imaginary axis as η varies, that is, if for any $\omega \in \mathbb{R}$, there is no η such that $\hat{g}(i\omega,\eta) = 0$. We note that if there exists an η such that $\hat{g}(i\omega,\eta) = 0$, then the line segment that is the set of all points between the end points of the two vectors $\hat{g}(i\omega,0)$ and $\hat{g}(i\omega,1)$ passes through the origin. This indicates that these two vectors point in opposite directions, i.e., $\phi(\omega) = \pm\pi$. Thus, we see that if condition (b) holds, then the stability of $\hat{g}(s,\eta)$ is maintained for $\eta \in [0,1/2) \cup (1/2,1]$. It can be concluded that condition (ii) is the same as condition (b) under the stated assumption.

The proof is completed by the fact that conditions (i) and (ii) are the same as conditions (a) and (b), respectively.

APPENDIX C: PROOF OF LEMMA 2

The scalar product of two vectors, $\hat{g}(i\omega,0)$ and $\hat{g}(i\omega,1)$, $\forall\omega \in \mathbb{R}$, in the complex plane is given by

$$\begin{aligned} F(k,\omega) &:= \mathrm{Re}[\hat{g}(i\omega,0)]\mathrm{Re}[\hat{g}(i\omega,1)] \\ &\quad + \mathrm{Im}[\hat{g}(i\omega,0)]\mathrm{Im}[\hat{g}(i\omega,1)] \\ &= (k-\mu)^2 + (\omega - a)^2 - k^2\Phi(\omega\delta)^2. \end{aligned}$$

If the delay amplitude δ and the coupling strength k are designed according to Lemma 1, then we have the inequality [33]

$$F(k,\omega) \geqslant \underline{F}(k,\omega) > 0, \tag{C1}$$

where

$$\underline{F}(k,\omega) := (k-\mu)^2 + (\omega - a)^2 - k^2\Gamma\left(\frac{\pi}{a}\omega\right),$$

$$\Gamma(x) := \begin{cases} -2(x-\pi)/(2+\pi), & x \leqslant \pi, \\ +2(x-\pi)/(2+\pi), & x \geqslant \pi. \end{cases}$$

It is known that the angle between two vectors is acute if their scalar product is positive. Thus, the inequality (C1) indicates that, in the complex plane, the angle $\psi(\omega)$ between the two vectors $\hat{g}(i\omega,0)$ and $\hat{g}(i\omega,1)$ satisfies

$$|\psi(\omega)| := |\arg[\hat{g}(i\omega,0)] - \arg[\hat{g}(i\omega,1)]| < \frac{\pi}{2}.$$

Therefore, $|\psi(\omega)| \neq \pm\pi$ holds for any $\omega \in \mathbb{R}$.

APPENDIX D: PROOF THAT $\mu - k < 0$

From Eqs. (17) and (19), it is obvious that the coupling strength k designed by Lemma 1 satisfies $\mu - k < 0$ if the function $h(\mu)$, defined as

$$h(\mu) := \max_{k\in[\bar{k}-\Delta k,\ \bar{k}+\Delta k]}\{\mu - k\} = \mu - (\bar{k} - \Delta k),$$

satisfies the inequality

$$h(\mu) < 0, \quad \forall\mu \in \left(0, \frac{a(2+\pi)}{4\pi}\right). \tag{D1}$$

Note that Δk, as defined by Eq. (20), is a function of μ. Let us consider the inequality (D1). It is straightforward to obtain

$$\begin{aligned} h(0) = 0, \quad \left.\frac{dh(\mu)}{d\mu}\right|_{\mu=0} &= 0, \\ \frac{dh(\mu)}{d\mu} < 0, \quad \forall\mu &\in \left(0, \frac{a(2+\pi)}{4\pi}\right). \end{aligned}$$

This shows that $h(\mu)$ is a monotonic decreasing function under Eq. (17), that is, the inequality (D1) holds. As a result, the coupling strength k designed by Lemma 1 always satisfies $\mu - k < 0$.

[1] A. Pikovsky, M. Rosenblum, and J. Kurths, *Synchronization* (Cambridge University Press, Cambridge, UK, 2001).
[2] G. Saxena, A. Prasad, and R. Ramaswamy, Phys. Rep. **521**, 205 (2012).
[3] A. Koseska, E. Volkov, and J. Kurths, Phys. Rep. **531**, 173 (2013).
[4] R. Herrero, M. Figueras, J. Rius, F. Pi, and G. Orriols, Phys. Rev. Lett. **84**, 5312 (2000).
[5] M. F. Crowley and I. R. Epstein, J. Phys. Chem. **93**, 2496 (1989).
[6] I. Ozden, S. Venkataramani, M. A. Long, B. W. Connors, and A. V. Nurmikko, Phys. Rev. Lett. **93**, 158102 (2004).
[7] K.-H. Ahn, J. R. Soc. Interf. **10**, 20130525 (2013).
[8] K. Bar-Eli, Physica D **14**, 242 (1985).
[9] D. G. Aronson, G. B. Ermentrout, and N. Kopell, Physica D **41**, 403 (1990).
[10] D. V. Ramana Reddy, A. Sen, and G. L. Johnston, Phys. Rev. Lett. **80**, 5109 (1998).
[11] D. V. Ramana Reddy, A. Sen, and G. L. Johnston, Physica D **129**, 15 (1999).
[12] D. V. Ramana Reddy, A. Sen, and G. L. Johnston, Phys. Rev. Lett. **85**, 3381 (2000).
[13] A. Prasad, Phys. Rev. E **72**, 056204 (2005).
[14] K. Konishi, Phys. Lett. A **341**, 401 (2005).
[15] R. Vicente, S. Tang, J. Mulet, C. R. Mirasso, and J.-M. Liu, Phys. Rev. E **73**, 047201 (2006).
[16] C. U. Choe, V. Flunkert, P. Hövel, H. Benner, and E. Schöll, Phys. Rev. E **75**, 046206 (2007).
[17] W. Zou and M. Zhan, Phys. Rev. E **80**, 065204 (2009).
[18] G. Saxena, A. Prasad, and R. Ramaswamy, Phys. Rev. E **82**, 017201 (2010).
[19] Y. N. Kyrychko, K. B. Blyuss, and E. Schöll, Eur. Phys. J. B **84**, 307 (2011).
[20] N. Punetha, R. Karnatak, A. Prasad, J. Kurths, and R. Ramaswamy, Phys. Rev. E **85**, 046204 (2012).
[21] W. Zou, D. V. Senthilkumar, Y. Tang, and J. Kurths, Phys. Rev. E **86**, 036210 (2012).
[22] W. Zou, Y. Tang, L. Li, and J. Kurths, Phys. Rev. E **85**, 046206 (2012).
[23] W. Zou, D. V. Senthilkumar, M. Zhan, and J. Kurths, Phys. Rev. Lett. **111**, 014101 (2013).
[24] W. Lin, Y. Pu, Y. Guo, and J. Kurths, Europhys. Lett. **102**, 20003 (2013).
[25] L. B. Le, K. Konishi, and N. Hara, Phys. Rev. E **87**, 042908 (2013).
[26] A. Prasad, Pramana-J. Phys. **81**, 407 (2013).
[27] A. Prasad, Y.-C. Lai, A. Gavrielides, and V. Kovanis, Phys. Lett. A **318**, 71 (2003).
[28] S. R. Huddy and J. D. Skufca, IEEE Trans. Power Electron. **28**, 247 (2013).
[29] D. Q. Wei, B. Zhang, X. S. Luo, S. Y. Zeng, and D. Y. Qiu, IEEE Trans. Circuits Syst. **60**, 692 (2013).
[30] T. Biwa, S. Tozuka, and T. Yazaki, Phys. Rev. Appl. **3**, 034006 (2015).
[31] F. M. Atay, Phys. Rev. Lett. **91**, 094101 (2003).
[32] K. Konishi, H. Kokame, and N. Hara, Phys. Rev. E **81**, 016201 (2010).
[33] K. Konishi, H. Kokame, and N. Hara, Phys. Lett. A **374**, 733 (2010).
[34] Y. Sugitani, K. Konishi, and N. Hara, Nonlin. Dyn. **70**, 2227 (2012).
[35] Y. Sugitani, K. Konishi, and N. Hara, in *Proceedings of the International Symposium on Nonlinear Theory and Its Applications* (IEICE, Tokyo, Japan, 2012), pp. 922–925.
[36] A. Gjurchinovski, A. Zakharova, and E. Schöll, Phys. Rev. E **89**, 032915 (2014).
[37] Y. Sugitani, K. Konishi, and N. Hara, in *Proceedings of the International Symposium on Nonlinear Theory and Its Applications* (IEICE, Tokyo, Japan, 2013), pp. 18–21.
[38] A. Gjurchinovski, Europhys. Lett. **84**, 40013 (2008).
[39] A. Gjurchinovski and V. Urumov, Rom. J. Phys. **58**, 36 (2013).
[40] W. Michiels, V. V. Assche, and S.-I. Niculescu, IEEE Trans. Autom. Control **50**, 493 (2005).
[41] F. M. Atay, J. Diff. Equ. **221**, 190 (2006).
[42] F. M. Atay and Ö. Karabacak, SIAM J. Appl. Dyn. Syst. **5**, 508 (2006).
[43] S. P. Bhattacharyya, H. Chapellat, and L. H. Keel, *Robust Control: The Parametric Approach* (Prentice Hall, Englewood Cliffs, NJ, 1995).
[44] A. Gjurchinovski and V. Urumov, Phys. Rev. E **81**, 016209 (2010).
[45] K. Pyragas, Phys. Lett. A **170**, 421 (1992).
[46] K. Konishi and N. Hara, Phys. Rev. E **83**, 036204 (2011).
[47] Y. Sugitani, K. Konishi, L. B. Le, and N. Hara, Chaos **24**, 043105 (2014).